

HIGH GAIN GAS MICROSTRIP DETECTORS FOR SOFT X-RAY DETECTION

J.E. Bateman, R. Barlow, G.E. Derbyshire, J.A. Mir and R. Stephenson

Rutherford Appleton Laboratory, Chilton, Didcot, Oxon, OX11 0QX, UK

23 August 2001

Abstract

This report describes development work in which systematic changes in the pitch of the electrode pattern of a Gas Microstrip Detector are explored in the search for higher avalanche gains and enhanced stability. With the cathode width set to half of the pitch, gas gains of $>50\,000$ are comfortably attainable with low detector noise so that x-rays can potentially be detected down to the limit of a single x-ray-produced photoelectron.

1. Introduction

Introduced a decade ago, the gas microstrip detector (GMSD) [1] was developed intensively over many years for demanding applications in Particle Physics collider experiments. In particular the ability of the GMSD to function at very high counting rates with long lifetimes while delivering sub-millimeter spatial resolution was demonstrated. This work is fully documented in the reports of the RD-28 programme [2,3]. The recent proliferation of Synchrotron Radiation (SR) sources with their very intense x-ray beams has stimulated interest in the possibilities of applying this now mature technology in the field of materials studies using SR beams. Applications in x-ray diffraction studies [4,5] and Extended X-ray Absorption Fine Structure (EXAFS) [6,7] have been reported. Most of the work centres on the detection of x-rays in the energy region 5-10keV for which the gas gain (≈ 2000) available from the standard GMSD design developed for Particle Physics applications is adequate. However, for sub-keV x-rays [7] the signal becomes marginal at such gains and a higher limiting gain is required. In surface EXAFS studies [8] it becomes necessary to use gas mixtures which do not give optimal gain conditions. In order to achieve adequate signals under such conditions, enhanced stability is required in the GMSD design.

Previous work [9] showed that for a given pitch of the electrode pattern the stable gain maximises for a cathode width of approximately half of the pitch. This report describes development work in which the pitch of the GMSD electrode pattern is systematically changed in the search for higher avalanche gains and enhanced stability, while the cathode width is fixed at 50% of the pitch. It is found that the pitch of the electrode structure does affect the detector stability. Over a reasonable range of pitch values (400microns – 800microns), gas gains of $>50\,000$ are comfortably attainable with low detector noise so that x-rays can be potentially detected down to the limit of a single x-ray-produced photoelectron. Avalanche gain saturation is observed with 5.9keV x-ray pulses for gains $>20\,000$.

2. GMSD Design and Operation

The GMSD patterns used in Particle Physics are geared towards maximum rate capability and high spatial resolution. A typical specification is: anode width 10 microns, cathode width 90 microns and pitch 300 microns. In a “good” gas mixture such as argon + 25% isobutane (or dimethylether) a maximum stable gain of up to 2000 can be achieved for a soft x-ray (for example Mn K at 5.9keV). When (for lower x-ray energies) helium is substituted for argon and a poorer quencher such as CO₂ is used, the maximum gain can drop to as low as 300, too low for comfortable operation. Studies at CERN showed that improved maximum gains of $\approx 15\,000$ could be obtained by using wider cathodes [10,11] but with relatively limited scope for optimisation. In reference [12] it is shown that wider pitches permit gains high enough for the detection of a single photoelectron. This study explores electrode designs with pitch values ranging between 300microns and 1200microns.

In order to explore the gain/stability question a special GMSD plate was fabricated with the following specification. There are seven sections each containing a number of strip patterns of a given pitch (constant within a section and varying between

0.3mm and 1.2mm between sections) with anodes of width 5 microns and the cathode width within a section set to 50% of the pitch. All the anodes and cathodes of a section are connected together so that an active area of approximately 6mm x 18mm is formed which is connected to the standard charge amplifier sensing circuit. The pitches of each section have the values: 300, 400, 500, 600, 800, 1000, 1200 microns (sections #7, #6, #5, #4, #3, #2, #1). The patterns are fabricated in 0.5 micron chromium on a 1mm thick plate of S8900 glass (50mm x 50mm). The plate is mounted in a gas-tight enclosure with a drift space of 10mm for x-ray conversion. For the tests reported, a gas mixture of argon + 25% isobutane is used throughout with a potential of -1400V applied to the drift electrode. The potential applied to the cathodes (V_c) is negative with the anodes at earth.

The anode width (5 microns) was chosen in the light of earlier results which showed that this value represents the optimum for gas gain in a GMSD structure [13].

3. Gain Measurements

The gas gain of each section was measured in the usual way by comparing the peak of the pulse height distribution generated by Mn K x-rays with a charge calibrator. An energy per ion pair of 27eV was assumed for the gas mixture. Figure 1 shows the set of gain versus V_c curves obtained from the seven sections. The maximum gain point in each set corresponds roughly to the maximum stable operating point in each case. Figure 2 shows a typical x-ray pulse height spectrum ($M=2939$). Figure 3 summarises the limiting gain parameters of the seven sections with the maximum gain (M_{max}) and the V_{cmax} rising as the electrode pitch increases. Figure 4 shows a plot of the energy resolution (relative FWHM) as a function of the gain for section #3. This is the typical response of a GMSD with an optimum resolution of $\approx 14\%$ for Mn K x-rays at medium gas gain ($500 < M < 3000$) with a slight deterioration at the highest gains. The energy resolution of all sections behaves in a similar manner with a FWHM $\approx 20\%$ near $M = M_{\text{max}}$.

4. Noise Measurements

Addressing the problem of detecting very low energy ($< 1\text{keV}$) x-rays, the key requirement is a low noise threshold as measured in terms of the energy deposit in the detector. This is quantified by defining a Noise Floor Energy (E_{NF}) such that the total noise counting rate above a threshold set at this energy is 10Hz. This rate is defined arbitrarily as well in excess of the cosmic ray background ($\approx 0.01\text{Hz}$), but, since the rise of the noise counting rate is extremely steep, large changes in the chosen rate cause little change to E_{NF} . The calibration of the energy scale was made by using the Mn K lines and their argon escape peaks. Since the typical values of E_{NF} are $< \approx 100\text{eV}$ and the lines are at 3000eV and 6000eV considerable extrapolation is required. It was found that provided the pulse height peaks were assigned the weighted energies of the Mn K_α and K_β lines (which are not resolved by the detector) extrapolated E_{NF} values could be calibrated down to $\approx 10\text{eV}$ with errors generally $< 10\%$ in E_{NF} .

Figure 5 shows E_{NF} plotted as a function of V_c for the detector section #3. As expected the noise floor decreases with increasing V_c (i.e. gas gain). E_{NF} easily reaches below 10eV, implying that single photoelectrons are potentially detectable.

A second measure of the system noise is available in the width of the charge calibration pulse height distribution. With $V_c=0$ this is just the amplifier noise which is expected to be dominated by the series noise generated by the section electrode capacitance and resistance combined with the corresponding parameters of the FET input of the preamplifier. Measurement shows that a typical section looks like a parallel capacitor of $\approx 20\text{pF}$ with a series resistance of 600 ohms. Figure 6 shows the measured pulser noise width and capacitance for each section. The variation of the noise with electrode pitch (in figure 6) tends to indicate that the noise is proportional to the section capacitance. This is consistent with the dominance of the series resistance noise term. The pulser noise shows no detectable variation with the V_c (i.e. gas gain) for any section.

5. Discussion

X-ray energy resolution and linearity

Figure 2 shows that for pitch values (P) of $400 < P < 800$ microns stable gains of approaching $M = 10^5$ are possible, permitting single photoelectron detection as reported in reference [12]. However as figure 4 shows, the x-ray energy resolution for 5.9keV x-rays degrades steadily for $M > 3000$. Investigating the x-ray pulse height spectra as a function of gain shows that considerable non-linearity and distortion is apparent at the higher gains. Figure 7 shows three 5.9keV x-ray pulse height spectra taken at gains of 2939, 49755 and 1.004×10^5 in section #3. They have all been area normalised (same number of events) and the two lower gain curves have been gain normalised to make the peaks coincide.

The first striking observation is that the highest gain spectrum ($M=10^5$) is dramatically distorted and showing signs of the onset of a non-linear process such as streamer amplification. The normalisation of the two lower gain spectra shows not only the broadening of the x-ray lines but also the relative movement of the argon escape and full energy peaks which indicates the onset of avalanche saturation. When the ratio of the full energy peak channel to the escape peak channel is plotted as a function of the gas gain, a rapid departure from the linear value of 2.0 is observed for $M > 20\,000$.

Noise

In the absence of noise generated by the detector, the noise floor energy is expected to be proportional to the white (electronic) noise divided by the avalanche gain. Figure 8 shows that for section #3 this is observed. A fit of E_{NF} to the function a/M is excellent with the measured values drifting slightly above the fit at the highest gain. Expressed in terms of the standard deviation (σ_e) of the pulser pulse height distribution, $a = 4.83\sigma_e$ or 2.05FWHM_e . This confirms the general rule-of-thumb that the useful noise

floor in a system dominated by white noise is just twice the FWHM of the pulser spectrum. In the most general terms:

$$E_{NF} = \frac{4.72w\sigma_e}{M} \quad (1)$$

where w is the energy per ion pair of the gas mixture.

Figure 8 shows how the noise floor energy of section #3 departs from this functional dependence at gains above 50 000. Figure 9 shows the noise pulse height distributions obtained from section #3 in this region. Below the critical value of V_c the noise distribution is just the gaussian of the white noise but as V_c increases two broadly peaked pulse distributions appear. At maximum gain ($V_c = -882.6V$) the peak of the strongest distribution occurs at a charge value of $\approx 7\,000$ electrons when the gain for an x-ray-generated electron is 10^5 . The implication of these observations is that the source of the electrons which are being amplified lies close to the anode so that the full amplification available from the drift region is not experienced. This could implicate a processing imperfection in the anode-cathode gap on the surface as the source of the excess noise signals. The variability between sections of the field-induced pulse spectra tends to implicate flaws in the processing as the likely sources.

The dependence of the pulser noise (σ_e) on the section capacitance yields a small benefit to the noise floor as the pitch is increased. However, the gain (M) is the dominant parameter in equation (1), making this benefit marginal.

6. Conclusions

Combined with the results of our previous measurements [9] the present tests show that if a GMSD pattern is constructed on S8900 glass with a 5micron wide anode, and the pitch of the pattern is selected between 400 and 800 microns with the cathode width set to 50% of the pitch, then in a suitable gas, stable gains of up to 10^5 are possible. For x-rays of several keV (e.g. Mn K) saturation of the gain process sets in above $M = 20\,000$, but operation appears to be stable to $M > 50\,000$.

For application to the detection of sub-keV x-rays it is important that this gain is achieved without the onset of gas-mediated noise processes. In the present case gains of $\approx 50\,000$ can be achieved with essentially only the electronic white noise present, giving useful noise floor energy of $< 10eV$ and potentially permitting the detection of single photoelectrons.

Acknowledgement

The GMSD plates were manufactured by Baumer IMT, Greifensee, Switzerland.

References

1. A. Oed, Nucl. Instr. and Methods **A263** (1988) 351
2. F. Sauli, RD-28 Status Report: Development of gas microstrip chambers for radiation detection and tracking at high rates, CERN/DRDC/93-34 (1993)
3. F. Sauli, Development of gas microstrip chambers for radiation detection and tracking at high rates, CERN/DRDC/94-45 (1995)
4. V. Zhukov, F. Udo, O. Marchena, F.G. Hartjes, F.D. van der Berg, W. Bras, E. Vlieg, Nucl. Instr. and Methods **A392** (1997) 83
5. J.E. Bateman, J.F. Connolly, G.E. Derbyshire, D.M. Duxbury, J. Lipp, J.A. Mir, R. Stephenson, J.E. Simmons and E.J. Spill, B.R.Dobson, R.C.Farrow, W. I. Helsby, R. Mutikainen and I. Suni, A Gas Microstrip Wide Angle X-ray Detector for Application in Synchrotron Radiation Experiments, Presented at the 5th International Conference on Position Sensitive Detectors, University College, London, 13-17 September 1999, to be published in Nucl. Instr. and Methods
6. A.D. Smith, J.E. Bateman, G.E. Derbyshire, D.M. Duxbury, J.D. Lipp, E.J. Spill and R. Stephenson, Nucl. Instr. and Method **A467** (2001) 1136-1139.
7. J.E. Bateman, G.E.Derbyshire, E.Dudzik, G. van der Laan, J.D.Lipp, A.D. Smith and R. Stephenson, Nucl. Instr. and Method **A467** (2001) 1140-1143; also J.E. Bateman, G.E.Derbyshire, E.Dudzik, G. van der Laan, J.D.Lipp, A.D. Smith and R. Stephenson, Rutherford Appleton Laboratory report, RAL-TR-2000-041 (<http://www-dienst.rl.ac.uk/library/2000/tr/raltr-2000041.pdf>), to be published in J. Sych. Rad.
8. T. Rayment, S.L.M. Schroeder, G.D. Moggridge, J.E. Bateman, G.E. Derbyshire and R. Stephenson, Rev. Sci. Instr. **71** (2000) 3640-3645
9. J.E.Bateman, R. Barlow, G.E.Derbyshire, J.A.Mir and R. Stephenson, Optimising the design of gas microstrip detections for soft x-ray detection, Rutherford Appleton Laboratory Report, RAL-TR-2001-008, (<http://www-dienst.rl.ac.uk/library/2000/tr/raltr-2000008.pdf>)
10. T. Beckers, R. Bouclier, Ch. Garabatos, G. Million, F. Sauli and L.I. Shekhtman, Nucl. Instr. and Method **A346** (1994) 95
11. R. Bouclier, M. Capeans, C. Garabatos, G. Manzin, G. Million, L. Ropelewski, F. Sauli, T. Temmel, L. Shekhtman, V. Nagaslaev, Yu. Pestov and A Kuleshov, Nucl. Instr. and Method **A365** (1995) 65
12. V. Peskov, B.D. Ramsey and P. Fonte, Nucl. Instr. and Method **A392** (1997) 89
13. J.E. Bateman, J.F. Connolly, G.E. Derbyshire, D.M. Duxbury, J. Lipp, J.A. Mir, R. Stephenson, J.E. Simmons and E.J. Spill, Studies of the gain properties of Gas Microstrip Detectors relevant to their application as X-ray detectors, Rutherford Appleton Laboratory Report, RAL-TR-1999-057, (<http://www-dienst.rl.ac.uk/library/1999/tr/raltr-1999057.pdf>) Presented at the International

Workshop on Micro-Pattern Gas Detectors, Orsay, France, 28-30 June 1999.

Figure Captions

1. Avalanche Gain versus V_c curves for the seven sections of the test detector. The line through the section #1 data is a model fit. The gas is argon + 25% isobutane and the drift electrode potential is $-1400V$.
2. Typical pulse height analyser spectra obtained with Mn K x-rays (^{55}Fe source) in section #3 of the detector at medium gain ($M=2939$).
3. The maximum stable gain achieved by each section (M_{max}) and the corresponding anode-cathode potential (V_c) as a function of the cathode width of the section.
4. The relative energy resolution (FWHM) of the Mn K x-ray lines as a function of the gas gain in a high gain section (#3). The ratio of the peak channels of the Mn K x-ray and argon escape lines is also plotted as a function of the gas gain.
5. The noise floor energy (E_{NF}) as a function of V_c for the detector section #3.
6. The RMS pulser noise (electrons) is plotted for each of the seven detector sections as a function of the pitch of the pattern, along with its measured capacitance.
7. The Mn K x-ray pulse height spectra observed in section #3 at medium, high and very high gas gain. The spectra are normalised as described in the text.
8. The noise floor energy plotted for section #3 as a function of the gas gain along with a fit of the form $N_{EF} = \text{constant}/M$.
9. The pulse height spectra of the noise pulses observed in section #3 as the gain is systematically increased.

FIGURE 1

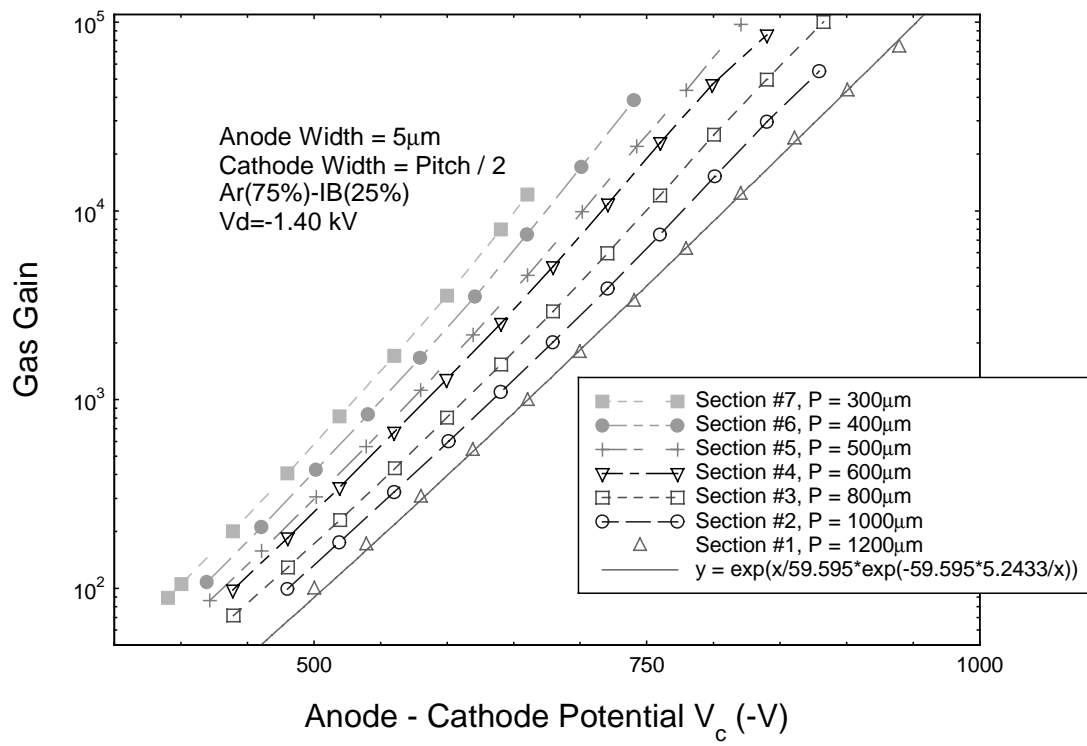


FIGURE 2

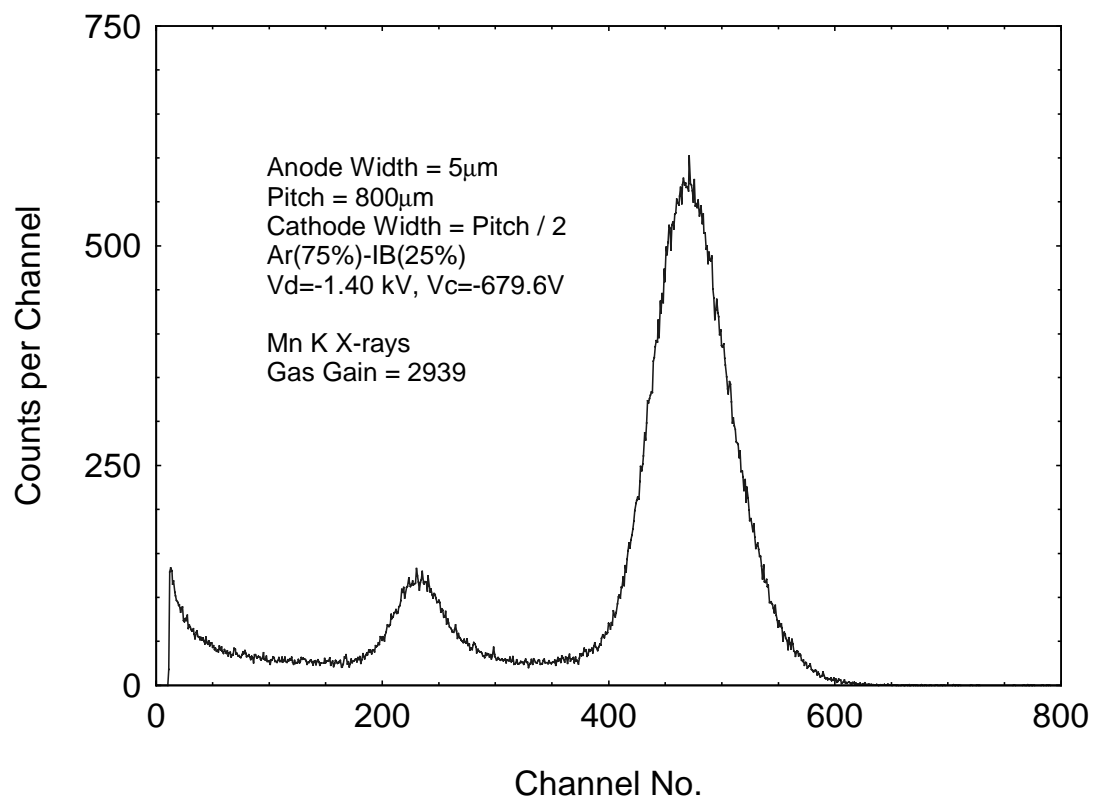


FIGURE 3

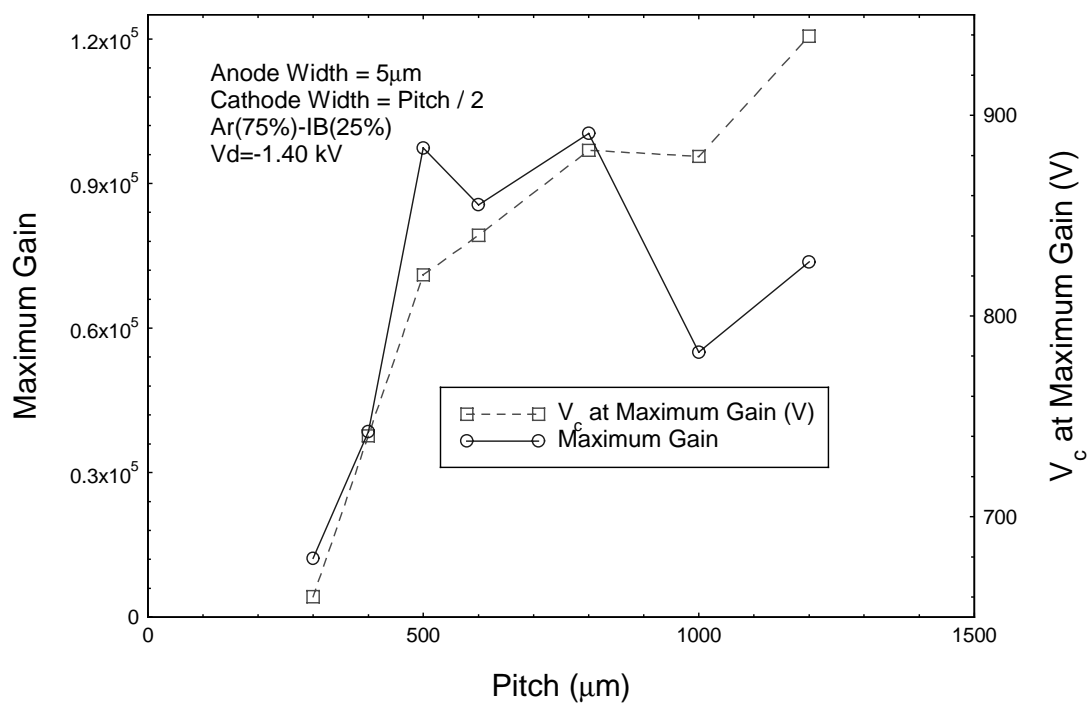


FIGURE 4

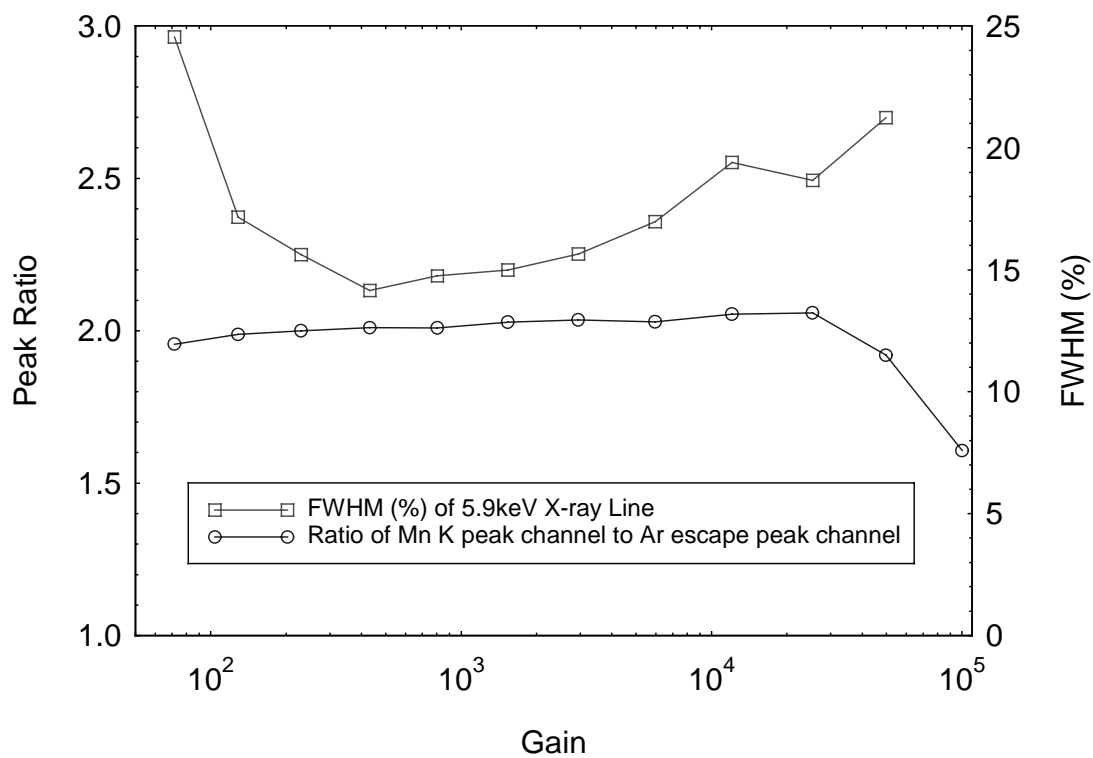


FIGURE 5

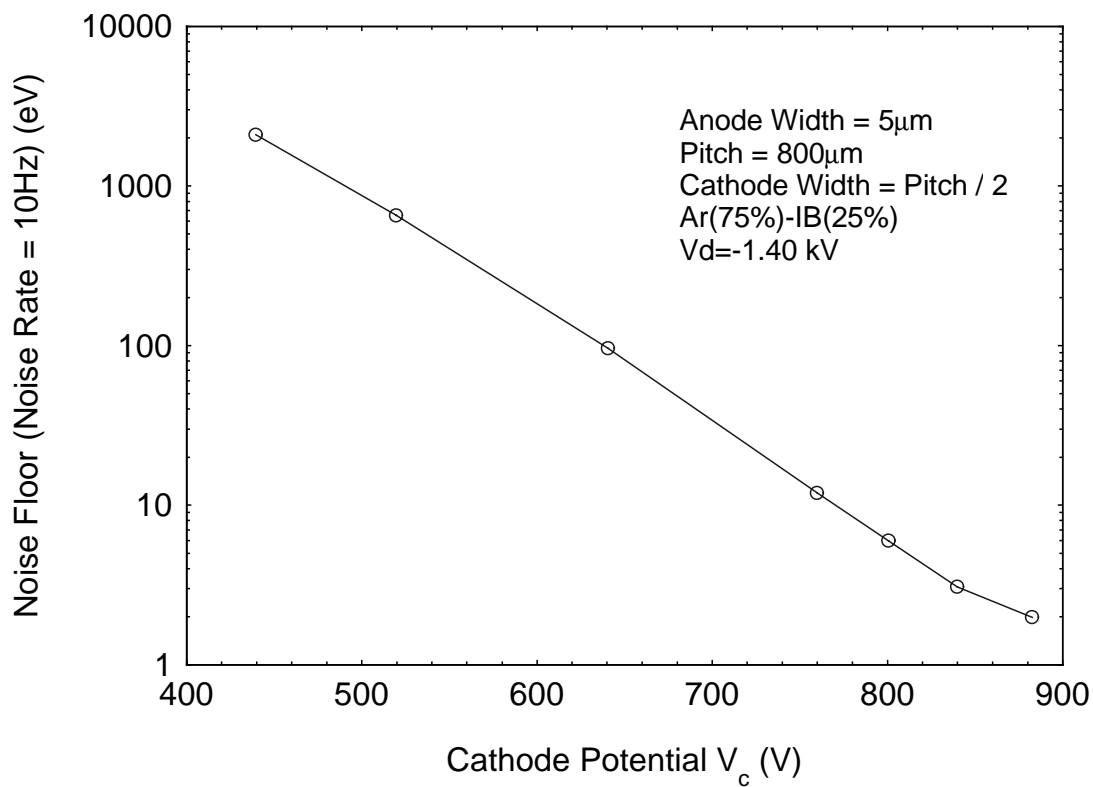


FIGURE 6

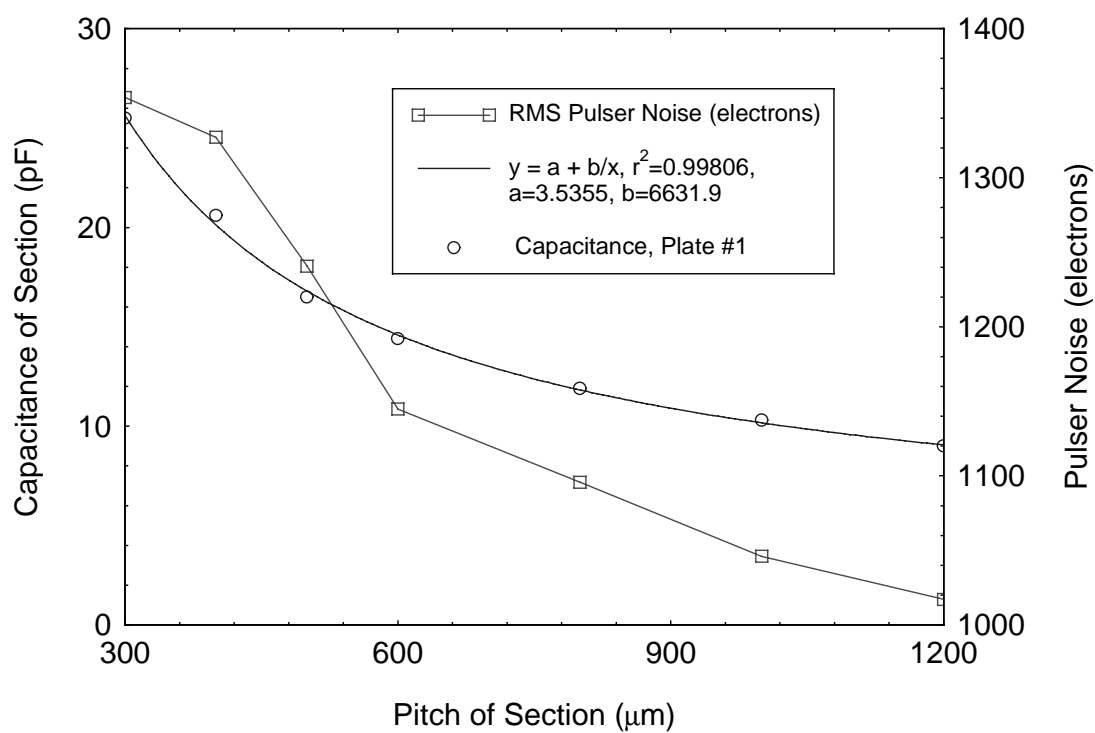


FIGURE 7

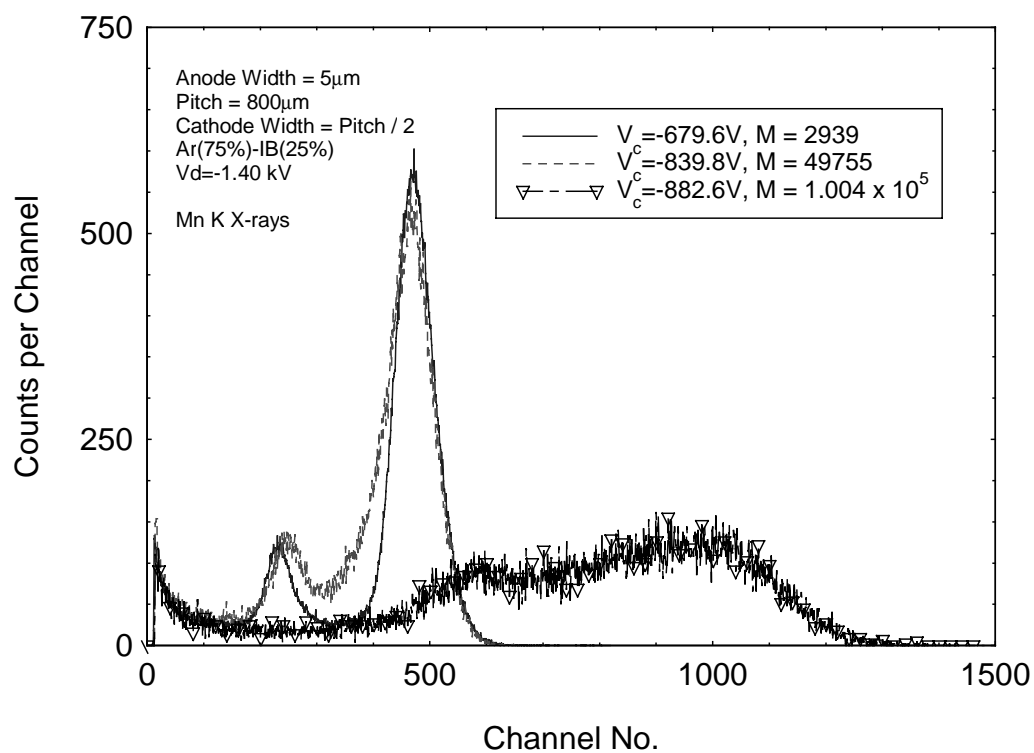


FIGURE 8

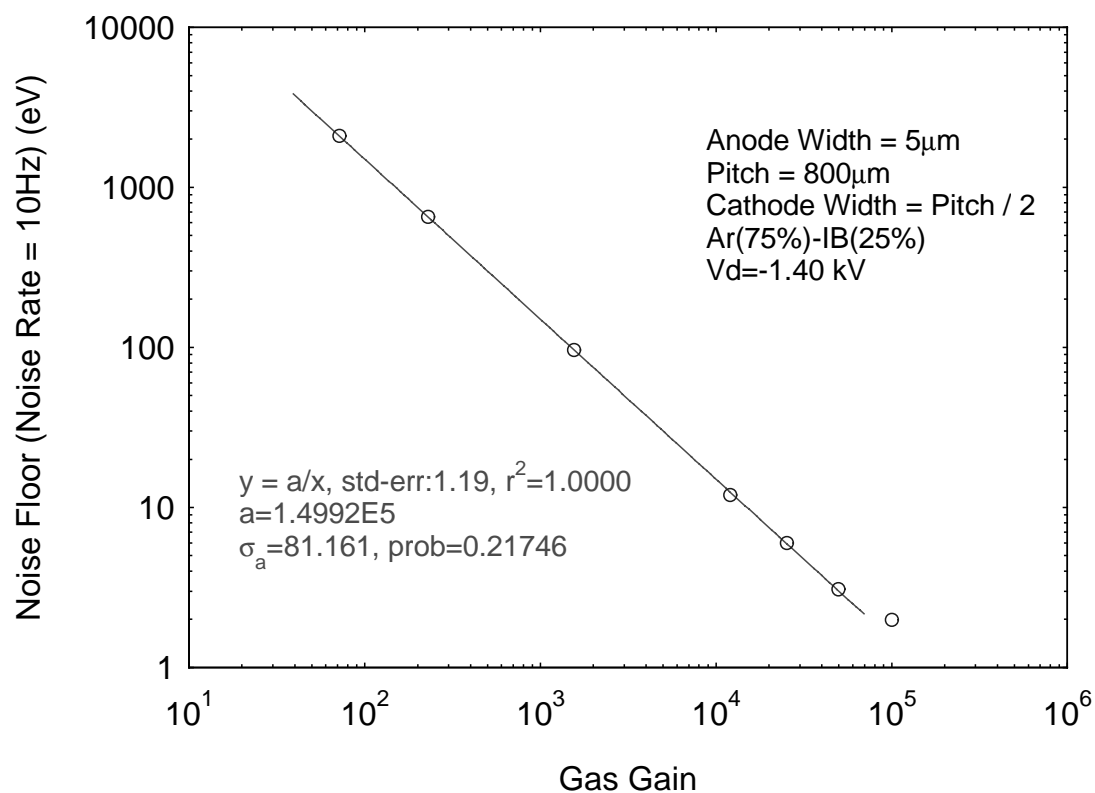


FIGURE 9

